HHS Public Access

Author manuscript

Dent Mater. Author manuscript; available in PMC 2021 March 01.

Published in final edited form as:

Dent Mater. 2020 March ; 36(3): 353–365. doi:10.1016/j.dental.2019.12.007.

Optimization of a real-time high-throughput assay for assessment of *Streptococcus mutans* metabolism and screening of antibacterial dental adhesives

Fernando Luis Esteban Florez[a,*], **Rochelle Denise Hiers**[a], **Yan Zhao**[b], **Justin Merritt**[c], **Adam Justin Rondinone**[d], **Sharukh Soli Khajotia**[a]

[a]The University of Oklahoma Health Sciences Center, Department of Restorative Sciences, Division of Dental Biomaterials, College of Dentistry, 1201 N. Stonewall Avenue, Oklahoma City, OK, 73117, USA

[b]The University of Oklahoma Health Sciences Center, Department of Biostatistics and Epidemiology, College of Public Health, 801 NE 13th Street, Oklahoma City, OK, 73126, USA

[c]Oregon Health & Science University, Department of Restorative Dentistry, School of Dentistry, MRB424, 3181 SW Sam Jackson Park Rd., Portland, OR, 97239, USA

[d]Oak Ridge National Laboratory, Center for Nanophase Materials Sciences, Oak Ridge, TN, 37831, USA

Abstract

Objective.—The present work shows the optimization of a high-throughput bioluminescence assay to assess the metabolism of intact *Streptococcus mutans* biofilms and its utility as a screening method for nanofilled antibacterial dental materials.

Methods.—The assay was optimized by monitoring changes in bioluminescence mediated by variation of the experimental parameters investigated (growth media and sucrose concentration, inoculum:D-Luciferin ratio, dilution factor, inoculum volume, luminescence wavelength, replicate and luciferase metabolic activity). Confocal microscopy was then used to demonstrate the impact of biofilm growth conditions on the 3-D distribution of extracellular polymeric substance (EPS) within *Streptococcus mutans* biofilms and its implications as confounding factors in high-throughput studies (HTS).

Results.—Relative Luminescence Unit (RLU) values from the HTS optimization were analyzed by multivariate ANOVA ($\alpha = 0.05$) and coefficients of variation, whereas data from 3-D structural parameters and RLU values of biofilms grown on experimental antibacterial dental adhesive resins

[*]*Corresponding author*. fernando-esteban-florez@ouhsc.edu (F.L. Esteban Florez).

Author contributions

FLEF and SSK conceptualized the study, analyzed the data and wrote the manuscript. RDH was responsible for the conduction of the experiment, data acquisition and data entry. YZ performed the statistical analysis of the HTS assay. AJR synthesized and functionalized the nanoparticles in dental adhesive resins. JM conceptualized the study, provided the bacterial strain and critically discussed the results. All authors have critically reviewed and approved the manuscript for publication.

Data availability statement

The datasets generated and analyzed during the current study are available from the corresponding author on reasonable request.

were analyzed using General Linear Models and Student–Newman–Keuls post hoc tests (α = 0.05). Confocal microscopy demonstrated that biofilm growth conditions significantly influenced the quantity and distribution of EPS within the 3-D structures of the biofilms. An optimized HTS bioluminescence assay was developed and its applicability as a screening method in dentistry was demonstrated using nanofilled experimental antibacterial dental adhesive resins.

Significance.—The present study is anticipated to positively impact the direction of future biofilm research in dentistry, because it offers fundamental information for the design of metabolic-based assays, increases the current levels of standardization and reproducibility while offering a tool to decrease intra-study variability.

Keywords

Bioluminescence; High-throughput; *Streptococcus mutans*; Dental adhesive resins; Antibacterial

1. Introduction

Bacterial viability is typically determined by counting the number of colony forming units (CFU) [1] using methodologies that are costly, labor-intensive, technique-sensitive and time consuming (ranging from 16 to 72 h) [2,3]. Another disadvantage associated with the CFU method is the level of biofilm manipulation required to separate bacteria from EPS within biofilms by vortexing, sonication or matrix-dissolving enzymes [4], which has been previously shown to impact cells' viability and leads to inaccurate viable cell counts. This, combined with the additional limitations mentioned, make these methodologies unsuitable for longitudinal HTS studies [2].

In this context, several assays capable of measuring bacterial viability based on metabolic reactions have been developed over the years [Crystal violet, Alamar Blue, 3-(4,5-dimethylthiazol-2-yl)-2,5-diphenyltetrazolium bromide (MTT) and 2,3-bis-(2-methoxy-4-nitro-5-sulfophenyl)-2h-tetrazolium-5-carboxanilide (XTT)]. However, despite many advantages reported in the literature [5], these types of metabolic assays typically require the utilization of large inocula (greater than 5- or 6-log CFU) and calibration curves derived from planktonic bacteria to successfully quantify the viability of bacteria in biofilms [2]. The latter requirement was demonstrated to introduce significant errors in the step of viability measurement due to marked differences in the metabolism of biofilms versus planktonic cells [1].

Optical density (OD) can be measured automatically in a HTS manner using a multi-well plate reader to estimate bacterial load. However, this method is limited to a concentration threshold between 10^8 and 10^{10} bacteria/mL, it is not capable of discerning between live/dead bacteria and suspended particulates and it is not technically feasible for intact biofilms. Other methods, such as confocal microscopy and flow cytometry, are less commonly used because they are time-consuming, require expensive equipment, trained personnel, and optical limitations restrict the efficiency of light collection to resolve subcellular structures [6]. These factors combined have decreased enthusiasm for the utilization of these methods in HTS studies. Therefore, robust, precise and repeatable assays are critically needed to

respond to recent expectations from the U.S. National Institutes of Health (NIH) for reproducible data [7].

Fluorescent and bioluminescent assays are based on the emission and collection of photons that are typically generated when molecules, excited either by light irradiation (fluorescence) or oxidation reactions (bioluminescence), transition to their corresponding fundamental states [6]. Due to their fundamental mechanisms, fluorescence assays are brighter, but display modest signal-to-noise ratios, which may adversely impact the sensitivity of these types of assays. In contrast, even though bioluminescence assays yield much lower light intensities, they also yield unrivaled signal-to-noise ratios, since photons are produced only from enzymatic reactions [8]. Therefore, bioluminescent assays are typically considered excellent candidates to generate meaningful data with the necessary throughput, quality, accuracy and specificity needed to translate biomolecular reactions into measurable parameters. According to Thorne et al. [8], these sophisticated assays are characterized by their ability to be translated into fully automated HTS systems capable of monitoring intricate biological processes.

Bioluminescent assays typically rely on the utilization of luciferase enzymes extracted from bioluminescence-producing organisms such as fireflies (*Photinus Pyralis*, 62-kDa; *Photuris pennsylvanica*, 61-kDa), click beetle (*Pyrophorus pla-giophthalamus*, 60-kDa), sea pansy (*Renilla reniformis*, 36-kDa) [6] and copepod (*Gaussia princeps,* 19-kDa) [9]. The underlying mechanism by which these structurally diverse enzymes are capable of oxidizing luciferins into oxyluciferins, with the concurrent emission of photons [10], has been previously described by the equation below by Shama and Malik [11], that describes the bioluminescence metabolic reaction for beetle luciferases such as firefly and click beetle.

$$Luciferin + O_2 + ATP \rightarrow Luciferin,$$
$$Mg^2 + Oxyluciferin + AMP + PPi + CO_2 + hv,$$

where ATP stands for adenosine triphosphate, AMP stands for adenosine monophosphate, PPi for pyrophosphate, and *hv* indicates emission of light.

Fan and Wood [6] have stated that luciferase reporter assays may be configured for HTS while providing a simple and efficient method to measure cellular physiological events without sacrificing data quality, due to signal amplification by intracellular transduction and genetic transcription pathways. Esteban Florez et al. [4] recently introduced and validated a non-destructive and real-time firefly assay based on a bacterial construct developed by Merritt et al. [12] The bioluminescent assay was demonstrated to be capable of assessing the viability of intact *Streptococcus mutans* biofilms grown on resin composites, and displayed strong Spearman correlation values for non-disrupted (r_s = 0.766, p < 0.0001) and soni-cated (r_s = 0.910, p < 0.0001) bacteria when compared to the CFU method [4]. Although the newly developed and validated assay has numerous advantages, it was based on a single-tube luminometer, lacked the necessary high-throughput and automation capabilities required for the analysis of large data sets in longitudinal studies with repeated measures. With this in mind, we present the optimization of a real-time and non-disruptive firefly bioluminescence assay capable of assessing, in a high-throughput manner, the metabolism of

non-disrupted cariogenic (caries-producing) biofilms. The optimized assay was then used to determine the impact of novel experimental dental adhesive resins containing either single-doped [nitrogen doping (N_TiO_2)] or co-doped titanium dioxide nanoparticles [nitrogen and fluorine doping (NF_TiO_2) or nitrogen and silver doping (Nag_TiO_2)] on the metabolism of intact *S. mutans* biofilms. The complete underlying mechanism of action of doped- or co-doped TiO_2 photocatalysis remains to be fully elucidated. However, the generation of reactive oxygen species (ROS) upon on-demand visible light irradiation (400–700 nm) along with lipid peroxidation are believed to be the major processes by which these nanoparticles express their antibacterial functionalities. Therefore, the rationale for the selection of these types of metaloxide nanoparticles was based on (i) the ability of nanoparticles to exert antibacterial properties when immobilized in current polymer compositions (in both dark and visible-light irradiated conditions), (ii) our ability to synthesize metaloxide nanoparticles using robust solvothermal reactions and (iii) a recent publication from our laboratory describing the antibacterial and bioactive properties of N_TiO_2 using viable colony counts (CFU/mL), live/dead staining, confocal microscopy and SEM/EDS, respectively [13].

2. Materials and methods

2.1. Bacterial strain and in vitro growth of biofilms

A genetically modified and bioluminescent strain of *Streptococcus mutans* (JM10), a derivative of wild type UA159 constructed by Merritt et al. [12] was used. Colonies of JM10 were grown on TH agar plates (Todd-Hewitt, BD Difco, USA) supplemented with 0.3% yeast extract (EMD Millipore, USA) and 800 μg/mL of Spectinomycin (MP Biomedicals, USA) under anaerobic conditions at 37 °C for 48 h for a total of two passages. A single colony was inoculated in 4.0 mL of THY broth with 32 μL of Spectinomycin (100 mg/mL), then incubated at 37 °C for 16 h (static cultures, anaerobic conditions). Planktonic cultures having optical densities (OD_{600}) equal to or higher than 0.900 (corresponding to 6.43 e^{+12} CFU/mL) were used for biofilm growth. Four dilutions of bacterial inoculum [1:50, 1:100, 1:250 and 1:500 (v/v)], three concentrations of THY biofilm growth media (0.35x, 0.65x, and 1x) and three concentrations of sucrose [0.1, 0.5, or 1.0% (w/v)] were the growth conditions tested. Each combination (inoculum + growth medium + sucrose) was then used to grow biofilms (n = 6/combination, total n = 10,368) in the wells of sterile white 24-well plates (catalog #6005816; Perkin-Elmer, USA) for either 24 or 48 h in anaerobic conditions at 37 °C, as described in Table 1.

2.2. Bioluminescence assay

After the growth period of either 24 or 48 h, biofilms were removed from the incubator, the media was aspirated and the biofilms were then washed twice with phosphate buffered saline (PBS, pH 7.4) for the removal of non-adherent cells following a modified protocol previously published by our laboratory. [14] Briefly, aliquots (1.0 mL/well) of room-temperature PBS were carefully dispensed into the wells containing biofilms using a serological pipette. Biofilms in PBS were then washed for 15 s at 150 revolutions per minute (RPM) using an orbital shaker (KS 260, IKA-Werke GmbH & Co. KG, Germany). After that, 1x THY + 1% glucose culture medium (recharge medium) was added to biofilms in the same volume as the original inoculum volume (either 300, 500, 750 or 1000 μL). Recharged

biofilms were then incubated (37 °C, 1 h) in preparation for bioluminescence testing. D-Luciferin aqueous solution (100 mM) suspended in 0.1 M citrate buffer (pH 6.0) was added by a computer-controlled system in a Synergy HT Multi-mode microplate reader (Biotek, USA) to the wells containing both the biofilms and recharge medium in either 5:1 or 2:1 ratio [(v/v) of inoculum:D-Luciferin]. The assessment of luciferase metabolic activity in non-disrupted *S. mutans* biofilms was evaluated in 2-min increments (6 min total) after the addition of D-Luciferin substrate at 530 and 590 nm. These two wavelengths were chosen to demonstrate the relationship between wavelength and RLU values.

2.3. Nanoparticles' synthesis

Nitrogen-doped TiO_2 nanoparticles (N_TiO_2) were synthesized via a 2-step process wherein the first step was the solvothermal synthesis of pure TiO_2 in a manner similar to Dinh et al. [15], and the second step was doping of the TiO_2 in a manner similar to Huo et al. [16] In the first step, a solution comprised of 1.7 g Ti(IV)-butoxide (Aldrich, 97%), 4.6 g ethanol (Decon Labs, 200 proof), 6.8 g oleylamine (Aldrich, 70%), and 7.1 g oleic acid (Aldrich, 90%) was prepared, then mixed with 20 mL of 4% H_2O in ethanol (18-MΩ Milli-Q; Decon Labs). This solution was then split into two aliquots (≈20 mL/aliquot). Each aliquot was then placed into a high-pressure reaction vessel (Paar Series 5000 Multiple Reactor System) and reacted at 180 °C for 24h. External magnetic field and Teflon-coated stir bars were used to stir the vessels. The reaction vessels were Teflon-lined. After reaching room temperature, the solutions were decanted and washed 3 times with anhydrous ethanol to remove extraneous surfactants. The pure TiO_2 nanoparticles were readily dispersible into 20–30 mL ethanol, but did not form clear solutions. In the doping step, a portion of the TiO_2 nanoparticles in ethanol were then reacted with equal volume of triethylamine (Aldrich, 99.5%) at 140 °C for 12 h in the high-pressure reaction vessel. Upon cooling, the now-doped N_TiO_2 particles were rinsed 3 times with anhydrous ethanol. The final N_TiO_2 nanoparticle solution was in ethanol, and the particles' concentration was determined gravimetrically (≈35 mg/mL).

2.3.1. Synthesis of Co-doped nanoparticles—Additionally, two other types of TiO_2 nanoparticles were synthesized and doped using variations of the first and second steps in Section 2.4 above. Variation 1: Nitrogen and Silver co-doping (Nag_TiO_2) was obtained by a single reaction based on step 1 above, with the inclusion of 5% Ag (based on Ti content) and 5% N, using silver acetlyacetonate and tetramethyl ammonium hydroxide as the dopant sources. Variation 2: Nitrogen and Fluorine co-doping (NF_TiO_2) was obtained by a single reaction based on step 1 above, with the inclusion of 5% F (based on Ti content) and 5% N, using ammonium fluoride as the dopant source. In both variations, the TiO_2 nanoparticles formed as usual with the dopants in place.

2.4. Specimen fabrication

Disk shaped specimens (n = 18/group; diameter = 6.00 mm, thickness = 0.50 mm) of unaltered OptiBond Solo Plus (Kerr Corp., OPTB), Adper Scotchbond (3 M ESPE, SCTB), Clearfil SE Protect (Kuraray Co., CLRF) and experimental dental adhesive resins [OPTB + 30% (v/v) of either N_TiO_2, Nag_TiO_2 or NF_TiO_2 (Oak Ridge National Laboratory, USA)] were fabricated, light cured (160 s/specimen, UltraLume 5, Ultradent Products, Inc., USA)

and UV-sterilized (254 nm, 800,000 μJ/cm^2, UVP Crosslinker, model CL-1000, UVP, USA). Specimens were then transferred to 24-well plates containing sterile ultrapure water (1000 μL/well) and were incubated at 37 °C for 24 h for the extraction of unreacted monomers.

2.5. Optimized HTS viability assessment of S. mutans biofilms on experimental antibacterial adhesive resins

Biofilms of *S. mutans* (JM10) were grown on the surfaces of specimens (n = 18/group) fabricated from unaltered (OPTB, SCTB, CLRF) and experimental dental adhesive resins containing 30% (v/v) of either N_TiO_2, NF_TiO_2 or Nag_TiO_2 to assess the impact of antibacterial materials on the viability of intact biofilms. Planktonic cultures of *S. mutans* (JM10) were grown in THY culture medium at 37 °C for 16 h. Planktonic cultures having optical density (OD_{600}) levels equal to or higher than 0.900 (corresponding to 6.43 e^{+12} CFU/mL) were used as inoculum to grow the biofilms. Optimal biofilm growth parameters identified during the HTS optimization [1:50 dilution, 0.65x THY + 1% (w/v) sucrose, 1000 μL] were then used to grow the biofilms. Aliquots (1.0 mL) of inoculated biofilm growth media were dispensed into the wells of sterile 24-well microtiter plates (Falcon, Corning, USA) containing sterile specimens. Biofilms were grown for either 24 or 48 h (static cultures, anaerobic conditions, 37 °C) with or without continuous light irradiation provided by a prototype LED device (410 ± 10 nm, 24-h irradiation = 310.07 J/cm^2, 48-h irradiation = 620.14 J/cm^2). An additional set of specimens fabricated with OPTB was treated with 2% chlorhexidine gluconate (CHX) for 2 min and served as the negative control group. After the growth period, biofilms were replenished with 1.0 mL of fresh 1x THY + 1% (w/v) glucose recharge medium and were incubated at 37 °C for 1 h. Replenished biofilms were transferred into the wells of sterile white 24-well plates containing 1.0 mL of fresh 0.65x THY + 1% (w/v) sucrose medium. D-Luciferin aqueous solution (100 mM) suspended in 0.1 M citrate buffer (pH 6.0) was added by a computer-controlled system in a Synergy HT Multi-mode microplate reader (Biotek, USA) to the wells containing both the specimens with biofilms and recharge medium in 2:1 ratio [(v/v) of inoculum:D Luciferin]. Luciferase metabolic activity in non-disrupted *S. mutans* biofilms was evaluated at 590 nm in 2-min increments (6 min total) after the addition of D-Luciferin substrate in terms of Relative Luminescence Units (RLUs).

2.6. Staining and confocal microscopy

A confocal microscopy assay was necessary to demonstrate the impact of biofilm growth conditions on the distribution of biofilm components nucleic acid, proteins and extracellular polymeric substances. To this end, an additional set of biofilms (n = 4/condition) were grown on sterile glass slides for 24 h using specific inoculum dilutions (1:50, 1:100, 1:250 and 1:500) and THY growth medium concentrations (0.35x, 0.65x and 1x) supplemented with 0.1% sucrose. Biofilms were then washed three times with PBS (pH 7.4, 25 °C, 15 s/wash) to remove non-adherent cells in preparation for concurrent staining with Alexa Fluor® 647 conjugate of Concanavalin A (Invitrogen, USA; 250 μg/mL), Syto 9 (Molecular Probes, USA; 10 μM), and Sypro Red (Invitrogen, USA; 10x), which are specific for the EPS, nucleic acid, and protein components of the biofilms, respectively, as described by Khajotia et al. [14] Biofilms were kept hydrated in sterile ultra-pure water and protected from light until confocal microscopy.

Biofilms were then imaged in sterile ultrapure water using a TCS-SP2 MP confocal laser scanning microscope (CLSM, Leica Microsystems, Inc., USA) with Ar (488 nm) and He/Ne (543 and 633 nm) lasers for excitation of the fluorescent stains. A 63x water immersion microscope objective lens was used. Serial optical sections were recorded from the top of glass slides to the top of the biofilms at 0.6 μm intervals in the z-direction. Four specimens were tested per group and three locations were scanned on each specimen, resulting in 12 CLSM images per group. Two 3-dimensional biofilm structural parameters [biovolume (BV) and mean biofilm thickness (MTBF)] were calculated for each biofilm component (fluorescent stain) using ISA3D software, as described by Khajotia et al. [14]. Representative 3-D images of the biofilms were generated using Volocity software (PerkinElmer, USA) to help with visualization of the distribution of the nucleic acid, proteins and EPS components of the biofilms.

2.7. Statistical analyses

RLU values obtained during the optimization of the HTS bioluminescence assay for each combination of experimental variables investigated shown in Table 1 (inoculum dilution [1:50, 1:100, 1:250 and 1:500], THY [0.35x, 0.65x, and 1x] and sucrose concentration [0.1, 0.5, or 1.0%]) were analyzed using multivariate ANOVA and coefficients of variation (CV). Data for each of the 3-D structural parameters (BV and MTBF) were analyzed using General Linear Models (GLM) and post hoc Student Newman Keuls tests (SNK; $\alpha = 0.05$). RLU values indicating the viability of intact biofilms of *S. mutans* grown against the surfaces of both unaltered and experimental dental adhesive resins were also compared using GLM and SNK *post hoc* tests ($\alpha = 0.05$). All statistical analyses were performed with the Statistical Analysis System (SAS software, version 9.2; SAS Institute, USA).

3. Results

The objective of this study was to optimize a real-time, non-destructive firefly bioluminescent assay introduced by Esteban Florez et al. [4] into a high-throughput methodology that can assess the metabolism of intact *S. mutans* biofilms grown on the surfaces of dental biomaterials with antibacterial functionalities or treated with antibacterial agents such as chlorhexidine gluconate. Table 1 illustrates the experimental conditions and parameters investigated during the optimization process that resulted in a total of 6,912 possible combinations of factors analyzed. Table 2 displays the Student–Newman–Keuls ranking describing the mean values of luciferase metabolic activity (in RLUs) and distribution of statistical significance among groups investigated for (A) 0 min, (B) 2 min, (C) 4 min and (D) 6 min after the addition of D-Luciferin substrate

Fig. 1 (A–H) illustrates the results from experimental parameters (A) media concentration, (B) sucrose concentration, (C) inoculum:D-Luciferin ratio, (D) dilution factor, (E) inoculum volume, (F) luminescence wavelength, (G) replicate, and (H) luciferase metabolic activity investigated during the optimization process. It is possible to observe that bioluminescence signals were significantly ($p < 0.001$) influenced by experimental parameters such as medium (0.35x, 0.65x or 1x) and sucrose concentration (0.1, 0.5 or 1.0 %), inoculum:D-Luciferin ratio (5:1 or 2:1), inoculum volume (300, 500, 750 or 1000 μL), wavelength (530

or 590 nm) and replicate (Week 1, 2 or 3), wherein RLU values increased directly with the variation of the parameter investigated. A significant ($p < 0.001$) but inverse relation was observed between RLU values and experimental parameters such as dilution factor (1:500, 1:250, 1:100 or 1:50) and luciferase metabolic activity (0, 2, 4 and 6 min).

Fig. 2 (A–L) illustrates representative 3-dimensional reconstructions of *S. mutans* biofilms evidencing the distribution of nucleic acids (green fluorescence), proteins (red fluorescence) and EPS (blue fluorescence), obtained with confocal laser scanning microscopy, in terms of growth medium concentration[0.35x (A–D), 0.65x (E–H) and 1.00x (I–L)] and dilution factor [1:500 (A, E, I), 1:250 (B, F, J), 1:100 (C, G, K) and 1:50 (D, H, L)].

Two 3-D parameters [biovolume (BV) and mean biofilm thickness (MTBF) related to the structure and composition of biofilms were analyzed. Fig. 3 shows the statistical analyses of the distribution of nucleic acids (NA), proteins (P) and EPS in function of BV and MTBF. The results reported in Fig. 3A have demonstrated that the mean BV of NA was significantly influenced by media concentration ($p = 0.0007$) and dilution factor ($p < 0.0001$). The distribution of NA in MTBF (Fig. 3B) was shown to be significantly influenced by growth medium concentrations ($p < 0.0001$), dilution factor ($p < 0.0001$) and by the interaction between factors ($p = 0.0010$). Fig. 3C demonstrates the results from the distribution of P within biofilms for BV, where it was observed that growth medium concentration ($p = 0.0001$) and dilution factor ($p < 0.0001$) significantly affected the composition of biofilms. Distribution of P for MTBF (Fig. 3D) was observed to be significantly influenced by growth medium concentration ($p = 0.0007$) and dilution factor ($p = 0.0106$). The results shown in Fig. 3E and F demonstrate the distribution of EPS in BV and MTBF, respectively, where It is possible to observe that EPS distribution within biofilms was significantly affected by media concentration and dilution factor in BV ($p = 0.0007$, $p < 0.0001$) and MTBF ($p < 0.0010$, $p < 0.0001$), respectively. The interaction between parameters was demonstrated to significantly affect EPS in MTBF ($p = 0.0010$) but not in BV ($p = 0.0630$). These findings have demonstrated that biofilm growth parameters such as inoculum dilution, growth media and sucrose concentration directly impact the quantity and 3-dimensional distribution of selected components within *S. mutans* biofilms, which in turn, may adversely impact the ability the assay reported to precisely screen the metabolism of *S. mutans* grown on relevant dental substrates. This observation is anticipated to positively impact the direction of future biofilm research in dentistry, because it offers fundamental information for the design of metabolic-based assays, increases the current levels of standardization and reproducibility while offering a tool to decrease intra-study variability.

Figs.4 and 5 show the results from the optimized bioluminescence HTS assay that was used to assess, in a real-time and non-destructive manner, the metabolism of intact *S. mutans* biofilms grown for either 24 or 48 h, with or without continuous visible light irradiation, on specimens of both unaltered (OPTB, SCTB, CLRF) and experimental dental adhesive resins containing metaloxide nanoparticles [OPTB + 30% (v/v) of either N_TiO_2, Nag_TiO_2 or NF_TiO_2]. It is possible to observe in Figs.4A and 5 A [Light Irradiated (24 and 48 h)] that biofilms grown on both unaltered and experimental dental adhesive resins, displayed metabolic levels that were comparable under continuous visible light irradiation for either 24 or 48 h as denoted by similar RLU mean values and the interaction between factors

(growth*light irradiation, p = 0.1218). Figs.4B and 5 B [Dark Conditions (24 and 48 h)] have demonstrated a consistent trend where SCTB and OPTB supported the growth of biofilms that displayed metabolic levels that were significantly ($p < 0.001$) higher amongst all groups tested, as denoted by the SNK rankings (Table 3) for luciferase metabolic activity (0, 2, 4 and 6 min) and higher bioluminescence signals (in RLUs) reported.

In addition, it was possible to observe that experimental materials containing 30% (v/v) of metaloxide nanoparticles supported biofilms whose metabolic levels were comparable to CLRF (fluoride-releasing material) as denoted by the SNK rankings (Table 3) and lower bioluminescence signals reported. It was also possible to observe that specimens fabricated with unaltered OPTB that were treated with CHX for two minutes demonstrated the lowest metabolic levels amongst all groups and conditions investigated.

4. Discussion

A preliminary search on PubChem [17] has demonstrated that from a total of 2000 assays currently listed, 74% are either bioluminescent or fluorescent in nature, which demonstrates the rising importance of bioluminescent assays for the scientific community [18]. Bioluminescent assays using beetle luciferases are based on a strong and linear relationship between internal ATP content and the emission of light [19], and may be characterized by their simplicity, sensitivity [quantum yield ≈ 90%, attomole range (10^{-18} mole)] and specificity (ATP-Mg^{2+}) [20]. Such proportional relationships have been observed in both eukaryotic and prokaryotic cells, and may be used to indicate not only the amount of viable cells present in a sample, but most importantly, to screen the efficacies of various antibacterial strategies in a high-throughput and real-time format [20].

Fan and Wood [6] have stated that ATP serves as a good indicator of cell viability because it is the major conduit of metabolic energy, and ATP concentrations are homeostatically maintained through a balance of generative and consumptive pathways. Sánchez et al. [21], while investigating the utility of a destructive ATP bioluminescence assay to assess the antimicrobial effects of mouthrinses (in vitro subgingival biofilm model), reported that bacterial load and cell viability were proportional to intracellular ATP content. The results reported in the present study are in agreement with previous studies, and have demonstrated that bioluminescence signals were proportional to growth medium concentration (0.35x, 0.65x and 1.00x), inoculum:D-Luciferin ratio (5:1 or 2:1) and inoculum volume (300, 500, 750 and 1,000 μL), whereby the highest mean bioluminescence signals (58,621 RLUs at 0 min) were observed for biofilms grown using 1x THY + 1% (w/v) sucrose (1000 μL and 2:1 innoculum:D-Luciferin ratio).

An inverse relationship was observed for parameters such as luciferase metabolic activity (0, 2, 4 and 6 min) and dilution factor (1:500, 1:250, 1:100 and 1:50). Such behavior can be partially explained by the typical intracellular degradation of D-Luciferin substrate over time. These results are corroborated by Loimaranta et al. [22] who have reported the typical decay of bioluminescence signals for a recombinant strain of *S. mutans* (0.6%/minute, at temperatures between 0 and 4 °C). The authors have also stated, based on previous scientific evidence [23], that bioluminescence assays performed at higher temperatures (room

temperature and 30 °C) should result in a rapid decrease in light emission [22]. The results of the present study suggest that bioluminescence assays conducted at oral temperature (37 °C) may not be suitable tools to assess the viability of intact *S. mutans* biofilms after long periods of time (15–30 min).

The levels of EPS deposition shown on Fig. 2D, G, K and L were hypothesized to result in limited D-Luciferin penetration and overall low bioluminescence signals, which would further explain the inverse relationship between dilution factor and bioluminescence, wherein a gradient of signal intensities was observed. These findings are corroborated by Zhang et al. [24] who have modeled, using the Stokes-Einstein equation, the effect of substrate size, electric charge and ionic strength on the diffusion coefficient of small molecules in a *S. mutans* biofilm model. According to their results, the diffusion coefficient of small molecules (such as D-Luciferin) tends to be inversely proportional to the molar masses of EPS components (dextrans and glucans). In addition to that, it is well-known that more concentrated inocula are typically associated with highly-heterogeneous biofilms due to starvation and cell death through the various layers of biofilms. These critical limitations are anticipated to result in bioluminescence assays that may not truly represent the total viable biomass in *S. mutans* biofilms grown for more than 48 h, due to their larger thickness, higher EPS contents and higher quantities of dead cells.

The results reported for the optimization of the high-throughput bioluminescence assay clearly indicates that biofilm growth parameters investigated (identified in Section 2.7 Statistical analyses as "*variables*"), directly impact the ability of the HTS assay to accurately screen the metabolism of *S. mutans* biofilms grown on relevant dental materials, such as the dental adhesive resins investigated in the present study. Since all experimental parameters (growth medium concentration, sucrose concentration, inoculum:D-Luciferin ratio, growth media dilution factor, inoculum volume, wavelength, replicate and luciferase metabolic activity) were shown to be significant predictors of response ($p < 0.001$), an analysis of the coefficient of variation (CV) of each combination of parameters was necessary to identify which experimental conditions would render bioluminescence signals with the necessary level of precision and repeatability to correctly determine the viability of intact *S. mutans* biofilms in a real-time and HTS format.

According to Reed et al. [25], this type of mathematical assessment provides a standard to determine if two assay results for the same subject, separated by an intervention, differ by more than expected from the intrinsic variation of the assay, thereby indicating an intervention effect. In this direction, experimental parameters (luciferase metabolic activity, in RLUs) with the lowest coefficient of variation (CV = 27.87%) included: (i) 0.65x THY, (ii) 1% (w/v) sucrose, (iii) 1:50 dilution factor, (iv) 1000 μL inoculum volume and (v) 2:1 inoculum:D-Luciferin ratio (500 μL). The optimized HTS bioluminescence assay was then used to determine the viability of *S. mutans* biofilms grown on the surfaces of unaltered (OPTB, SCTB, CLRF) and experimental dental adhesive resins containing 30% (v/v) of either N_TiO_2, Nag_TiO_2 or_NF TiO_2.

The results reported in Figs.4 and 5 suggest that biofilms grown under continuous visible light irradiation were associated with bioluminescence signals that were significantly lower

($p < 0.001$) than those of biofilms grown in dark conditions, which suggests that visible light irradiation has adversely impacted the viability of *S. mutans* biofilms in a material-independent manner. Our findings are corroborated by De Sousa et al. [26], and other reports [27–29], who have demonstrated that visible light irradiation remarkably impacted both the structure and viability of biofilms, by interfering with the ability of *S. mutans* to produce soluble and insoluble components of the EPS, thereby resulting in less viable, highly porous and structurally abnormal biofilms.

It is also possible to note in Figs.4B and 5 B that experimental dental adhesive resins containing 30% (v/v) of metaloxide nanoparticles (N_TiO_2, NF_TiO_2 and Nag_TiO_2) supported biofilms with metabolism levels that were significantly lower when compared to those grown either on unaltered OPTB or SCTB, and were similar when compared to unaltered CLRF (fluoride-releasing) in dark conditions, which was unexpected because N_TiO_2 is a photocatalyst that requires exposure to visible light irradiation to generate reactive oxygen species. These results indicate that the nanotechnology developed in our laboratory has a strong potential to be translated into commercial products capable of sustaining strong non-leaching antibacterial effects without light irradiation. Moreover, our results have also indicated that specimens fabricated with OPTB, that were subjected to treatment with CHX for 2 min, displayed the lowest viability levels amongst all groups tested, independent of light irradiation (with or without) or biofilm growth period (24 or 48 h). These findings can be explained by the experimental design proposed, where biofilms were treated with CHX prior to bioluminescence readings. Since CHX is a strong antibacterial agent against single-species biofilms in in vitro experiments, no discernible metabolic changes could be observed among the conditions tested. These results are in agreement with numerous publications demonstrating the utility of CHX as a powerful and broad-spectrum antibacterial agent in dentistry [30–33]. The present study has demonstrated the optimization of a real-time bioluminescence assay into a high-throughput assay that is capable of indirectly quantifying the viability of intact *S. mutans* biofilms by assessing their metabolic status. In addition, the present study demonstrated the utility of the optimized HTS bioluminescence assay to screen the antibacterial efficacies of polymeric restorative dental biomaterials and 2% chlorhexidine gluconate. The present study has also reported experimental nanofilled dental adhesive resins with promising non-leaching antibacterial properties. We propose that this HTS bioluminescence assay is a more desirable approach to determine the metabolism of intact cariogenic biofilms and to screen the efficacies of different antibacterial strategies in dentistry when compared to traditional assays previously described. When compared to previously reported assays [4,5,34–36], the present study is innovative because it allows for the real-time and precise screening of *S. mutans* metabolism and assesses the efficacy of antibacterial approaches displaying very different mechanisms of action (e.g., CHX, fluoride and ROS). In addition, the assay reported does not require the utilization of expensive equipment (e.g., confocal microscope, SEM, HPLC, MALDI-ToF) nor highly trained professionals, and requires minimal biofilm handling and manipulation. The assay is associated with unprecedented levels of throughput in dentistry and allows for high levels of intra-study standardization and reproducibility. It is anticipated that other studies will be conducted to allow the utilization of the optimized assay in multi-species biofilms grown on the surfaces of different dental biomaterials.

5. Conclusions

The present study successfully reported the optimization of an HTS real-time bioluminescent assay to quantify the viability of intact *S. mutans* biofilms, and the utility of the optimized assay to screen the antibacterial efficacies of unaltered and experimental dental adhesive resins containing metaloxide nanoparticles. The nanotechnology reported has the potential to increase the service lives of adhesive restorations by imparting promising non-leaching antibacterial properties to currently available polymer compositions.

Acknowledgments

The research results discussed in this publication were made possible in part by funding through the award project number HR16–131, from the Oklahoma Center for the Advancement of Science and Technology. The present work was also partially funded by the Oklahoma Shared Clinical and Translational Resources grant number NIGMS U54GM104938. The synthesis and characterization of metaloxide nanoparticles was conducted at the Center for Nanophase Materials Sciences (CNMS2013-331 and CNMS2015-331), which is a DOE Office of Science user facility. JM is funded by N.I.HNIDCR grants DE018893 and DE022083.

REFERENCES

[1]. Welch K, Cai Y, Strømme M. A method for quantitative determination of biofilm viability. J Funct Biomater 2012;3:418–31. [PubMed: 24955541]

[2]. Hazan R, Que Y-A, Maura D, Rahme LG. A method for high-throughput determination of viable bacteria cell counts in 96-well plates. BMC Microbiol 2012;12:259. [PubMed: 23148795]

[3]. Nybond S, Karp M, Tammela P. Antimicrobial assay optimization and validation for HTS in 384-well format using a bioluminescent *E. Coli* K-12 strain. Eur J Pharm Sci 2013;49:782–9. [PubMed: 23747659]

[4]. Esteban Florez FL, Hiers RD, Smart K, Kreth J, Qi F, Merritt J, et al. Real-time assessment of *Streptococcus mutans* biofilm metabolism on resin composite. Dent Mater 2016;32:1263–9. [PubMed: 27515531]

[5]. Mariscal A, Lopez-Gigosos RM, Carnero-Varo M, Fernandez-Crehuet J. Fluorescent assay based on resazurin for detection of activity of disinfectants against bacterial biofilm. Appl Microbiol Biotechnol 2009;82:773–83. [PubMed: 19198831]

[6]. Fan F, Wood KV. Bioluminescent assays for high-throughput screening. Assay Drug Dev Technol 2007;5:127–36. [PubMed: 17355205]

[7]. Lin NJ. Biofilm over teeth and restorations: what do we need to know? Dent Mater 2017;33:667–80. [PubMed: 28372810]

[8]. Thorne N, Inglese J, Auld DS. Illuminating insights into firefly luciferase and other bioluminescent reporters used in chemical biology. Chem Biol 2010;17:646–57. [PubMed: 20609414]

[9]. Goerke AR, Loening AM, Gambhir SS, Swartz JR. Cell-free metabolic engineering promotes high-level production of bioactive *Gaussia princeps* luciferase. Metab Eng 2008;10:187–200. [PubMed: 18555198]

[10]. Marques SM, Esteves da Silva JC. Firefly bioluminescence: a mechanistic approach of luciferase catalyzed reactions. IUBMB Life 2009;61:6–17. [PubMed: 18949818]

[11]. Shama G, Malik DJ. The uses and abuses of rapid bioluminescence-based ATP assays. Int J Hyg Environ Health 2013;216:115–25. [PubMed: 22541898]

[12]. Merritt J, Kreth J, Qi F, Sullivan R, Shi W. Non-disruptive, real-time analyses of the metabolic status and viability of *Streptococcus mutans* cells in response to antimicrobial treatments. J Microbiol Methods 2005;61:161–70. [PubMed: 15722141]

[13]. Esteban Florez FL, Hiers RD, Larson P, Johnson M, O'Rear E, Rondinone AJ, et al. Antibacterial dental adhesive resins containing nitrogen-doped titanium dioxide nanoparticles. Mater Sci Eng C 2018;93:931–43.

[14]. Khajotia SS, Smart KH, Pilula M, Thompson DM. Concurrent quantification of cellular and extracellular components of biofilms. J Vis Exp 2013:e50639. [PubMed: 24378651]

[15]. Dinh CT, Nguyen TD, Kleitz F, Do TO. Shape-controlled synthesis of highly crystalline titania nanocrystals. ACS Nano 2009;3:3737–43. [PubMed: 19807108]

[16]. Huo Y, Bian Z, Zhang X, Jin Y, Zhu J, Li H. Highly active TiO2-xNx visible photocatalyst prepared by N-doping in Et3N/EtOH fluid under supercritical conditions. J Phys Chem C 2008;112:6546–50.

[17]. Kim S, Thiessen PA, Bolton EE, Chen J, Fu G, Gindulyte A, et al. PubChem substance and compound databases. Nucleic Acids Res 2016;44:D1202–13. [PubMed: 26400175]

[18]. Inglese J, Thorne N, Auld DS. Reply to Peltz et al: post-translational stabilization of the firefly luciferase reporter by PTC124 (Ataluren). Proc Natl Acad Sci 2009;106:E65.

[19]. Fazilat S, Sauerwein R, McLeod J, Finlayson T, Adam E, Engle J, et al. Application of adenosine triphosphate-driven bioluminescence for quantification of plaque bacteria and assessment of oral hygiene in children. Pediatr Dent 2010;32:195–204. [PubMed: 20557702]

[20]. Brovko L. Bioluminescence and fluorescence for in vivo imaging. Bellingham, Washington, USA: Society of Photo-Optical Instrumentation Engineers, SPIE.

[21]. Sánchez MC, Llama-Palacios A, Marín MJ, Figuero E, León R, Blanc V, et al. Validation of ATP bioluminescence as a tool to assess antimicrobial effects of mouthrinses in an in vitro subgingival-biofilm model. Med Oral Patol Oral Cir Bucal 2013;18:e86–92. [PubMed: 23229259]

[22]. Loimaranta V, Tenovuo J, Koivisto L, Karp M. Generation of bioluminescent *Streptococcus mutans* and its usage in rapid analysis of the efficacy of antimicrobial compounds. Antimicrob Agents Chemother 1998;42:1906–10. [PubMed: 9687382]

[23]. Greger JE, Eisenberg AD. Adenosine 5'-triphosphate content of Streptococcus mutans GS-5 during starvation in a buffered salt medium. Caries Res 1985;19:314–9. [PubMed: 3861252]

[24]. Zhang Z, Nadezhina E, Wilkinson KJ. Quantifying diffusion in a biofilm of *Streptococcus mutans*. Antimicrob Agents Chemother 2011;55:1075–81. [PubMed: 21189346]

[25]. Reed GF, Lynn F, Meade BD. Use of coefficient of variation in assessing variability of quantitative assays. Clin Diagn Lab Immunol 2002;9:1235–9. [PubMed: 12414755]

[26]. De Sousa DL, Lima RA, Zanin IC, Klein MI, Janal MN, Duarte S. Effect of twice-daily blue light treatment on matrix-rich biofilm development. PLoS One 2015;10.

[27]. Araujo NC, Fontana CR, Bagnato VS, Gerbi ME. Photodynamic effects of curcumin against cariogenic pathogens. Photomed Laser Surg 2012;30:393–9. [PubMed: 22693952]

[28]. Chebath-Taub D, Steinberg D, Featherstone JD, Feuerstein O. Influence of blue light on *Streptococcus mutans* re-organization in biofilm. J Photochem Photobiol B Biol 2012;116:75–8.

[29]. Feuerstein O, Moreinos D, Steinberg D. Synergic antibacterial effect between visible light and hydrogen peroxide on *Streptococcus mutans*. J Antimicrob Chemother 2006;57:872–6. [PubMed: 16533827]

[30]. Ccahuana-Vásquez RA, Cury JA. S. mutans biofilm model to evaluate antimicrobial substances and enamel demineralization. Braz Oral Res 2010;24:135–41. [PubMed: 20658029]

[31]. Uzer Celik E, Tunac AT, Ates M, Sen BH. Antimicrobial activity of different disinfectants against cariogenic microorganisms. Braz Oral Res 2016;30:e125. [PubMed: 27901206]

[32]. Li X, Hoogenkamp MA, Ling J, Crielaard W, Deng DM. Diversity of *Streptococcus mutans* strains in bacterial interspecies interactions. J Basic Microbiol 2014;54: 97–103. [PubMed: 23456658]

[33]. da Silva TM, Alves FRF, Lutterbach MTS, Paiva MM, Ferreira DC. Comparison of antibacterial activity of alexidine alone or as a final irrigant with sodium hypochlorite and chlorhexidine. BDJ Open 2018;4:18003. [PubMed: 29868242]

[34]. Gerhardt PMRGE Wood WA, Krieg NR. Methods for general and molecular bacteriology. Washington, DC: American Soceity for Microbiology; 1994.

[35]. Hazan R, Que Y-A, Maura D, Rahme L. A method for high-throughput determination of viable bacteria cell counts in 96-well plates. BMC Microbiol 2012;12:259. [PubMed: 23148795]

[36]. Shiloh MU, Ruan J, Nathan C. Evaluation of bacterial survival and phagocyte function with a fluorescence-based microplate assay. Infect Immun 1997;65:3193–8. [PubMed: 9234774]

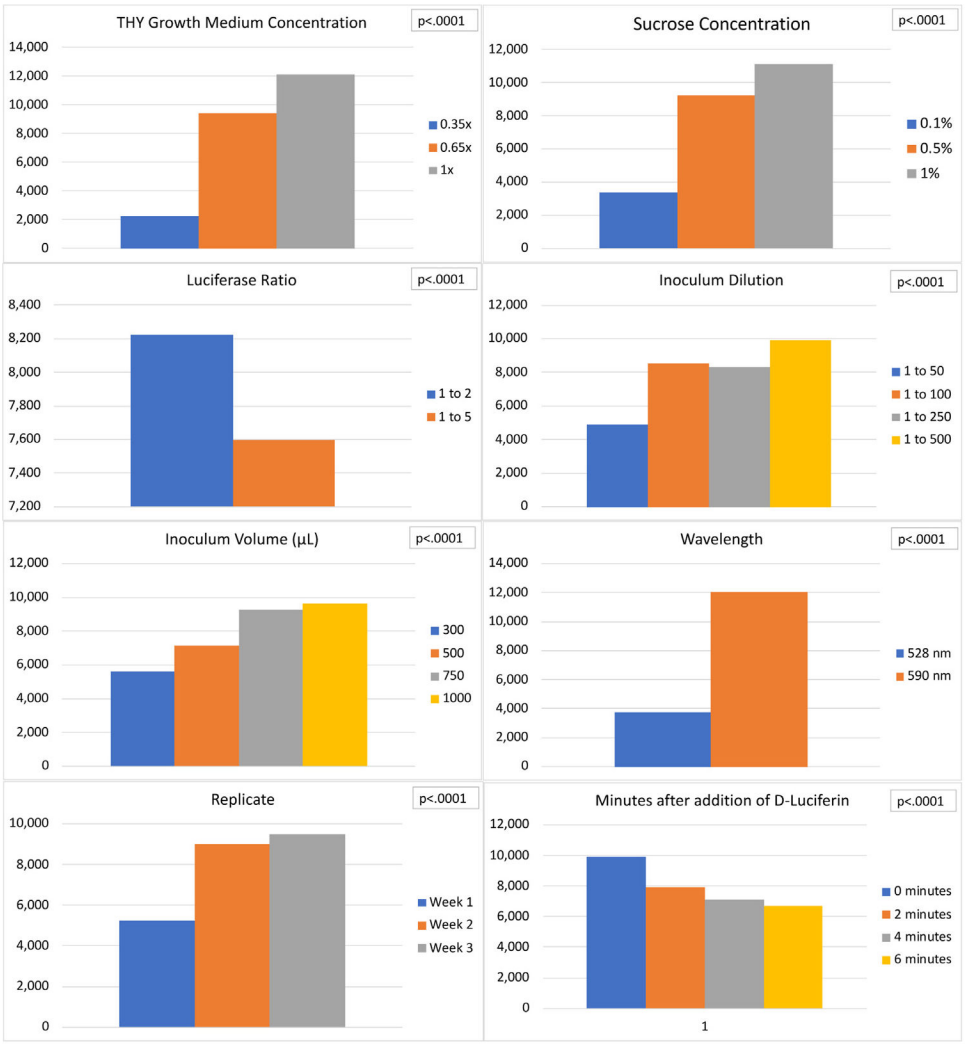

Fig. 1 –.

Results from the ANOVA test demonstrating the impact of (A) growth medium concentration (0.35x, 0.65x and 1x),(B) sucrose concentration (0.1%, 0.5% and 1%), (C) Luciferin to inoculum ratio (1:2 or 1:5), (D) dilution factor (1:500, 1:250, 1:100 and 1:50), (E) inoculum volume (300 µL, 500 µL, 750 µL and 1000 µL), (F) wavelength (530 nm or 590 nm), (G) replicate (Week 1, 2, 3) and (H) luciferase metabolic activity (0, 2, 4, 6 min). LS-Means stands for Least Squares means, which are means computed based on a linear model such as ANOVA.

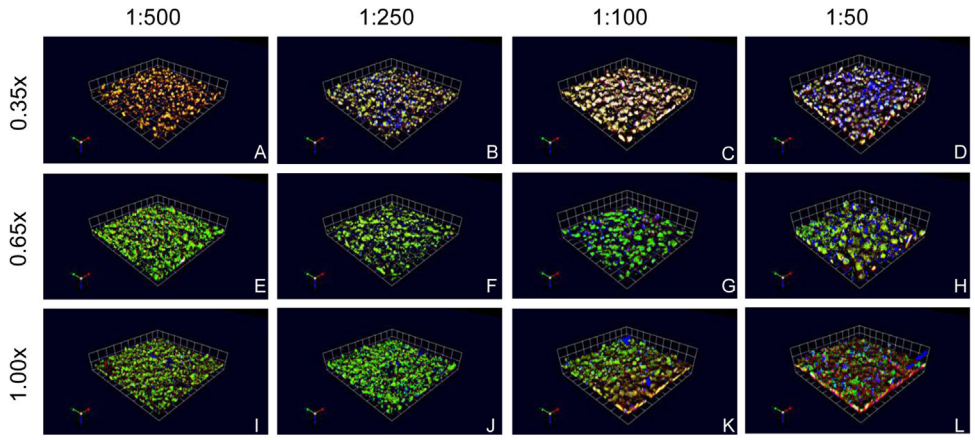

Fig. 2 –.

Representative 3-D reconstructions demonstrating the distribution of nucleic acids (green fluorescence), proteins (red fluorescence) bacterial and EPS (blue fluorescence) within biofilms grown on glass slides using selected growth medium concentrations [0.35x (A–D), 0.65x (E–H) and 1.00x (I–L)] and dilution factors [1:500 (A, E, I), 1:250 (B, F, J), 1:100 (C, G, K) and 1:50 (D, H, L)] of THY growth medium supplemented with 0.1% (w/v) sucrose (For interpretation of the references to colour in the figure legend and text, the reader is referred to the web version of this article).

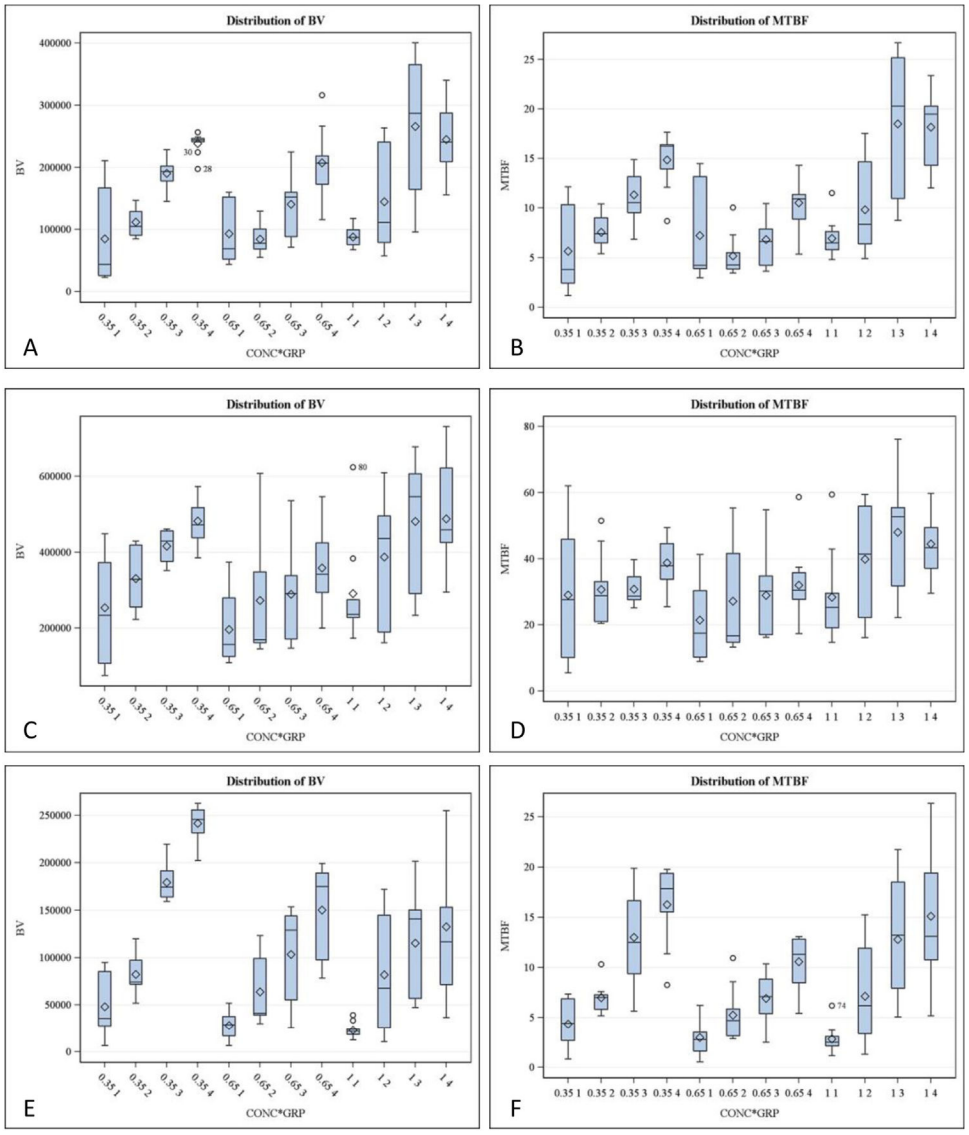

Fig. 3 –.

Distribution of nucleic acids, proteins and EPS in function of the two 3-D structural parameters (BV and MTBF) investigated.

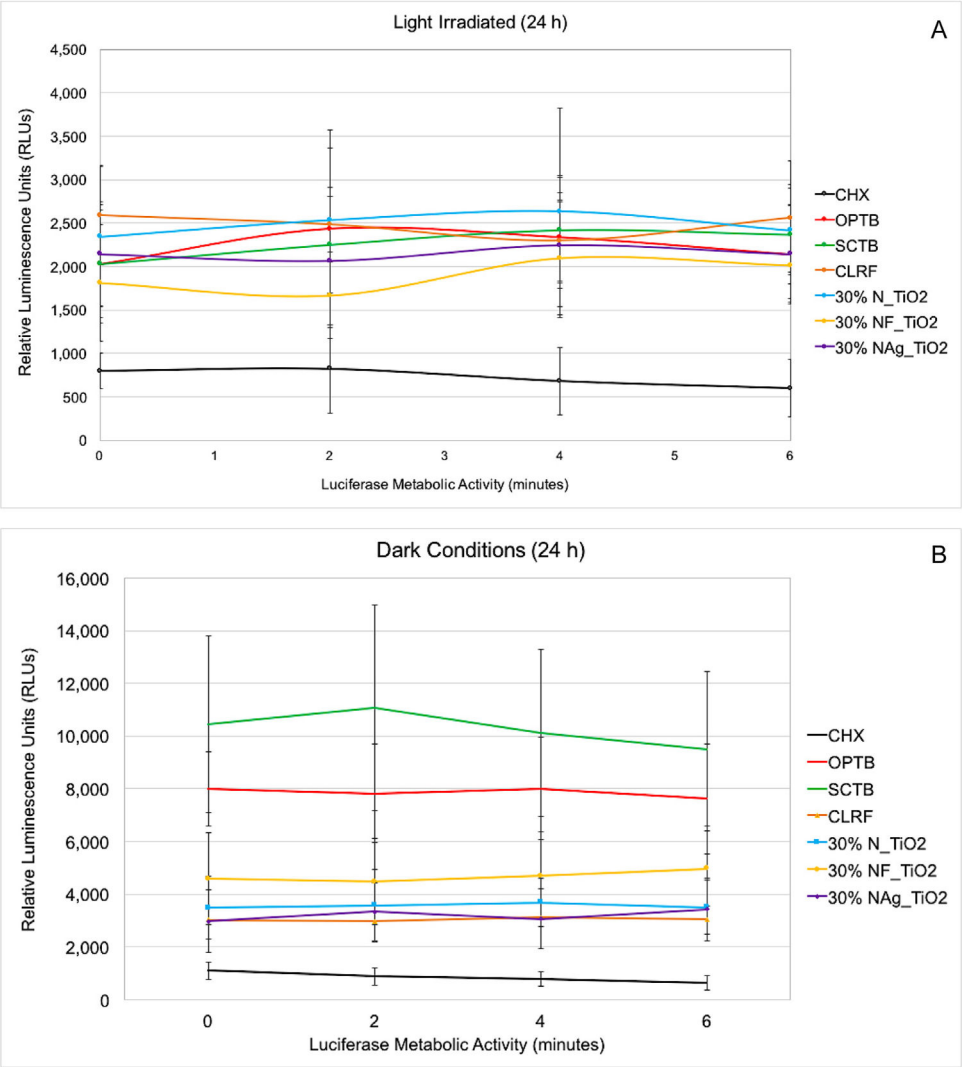

Fig. 4 –.

Viability of 24-h intact *S. mutans* biofilms grown against the surfaces of both unaltered and experimental dental adhesive resins containing 30% (v/v) of either doped or co-doped metaloxide nanoparticles (A) with or (B) without continuous light irradiation.

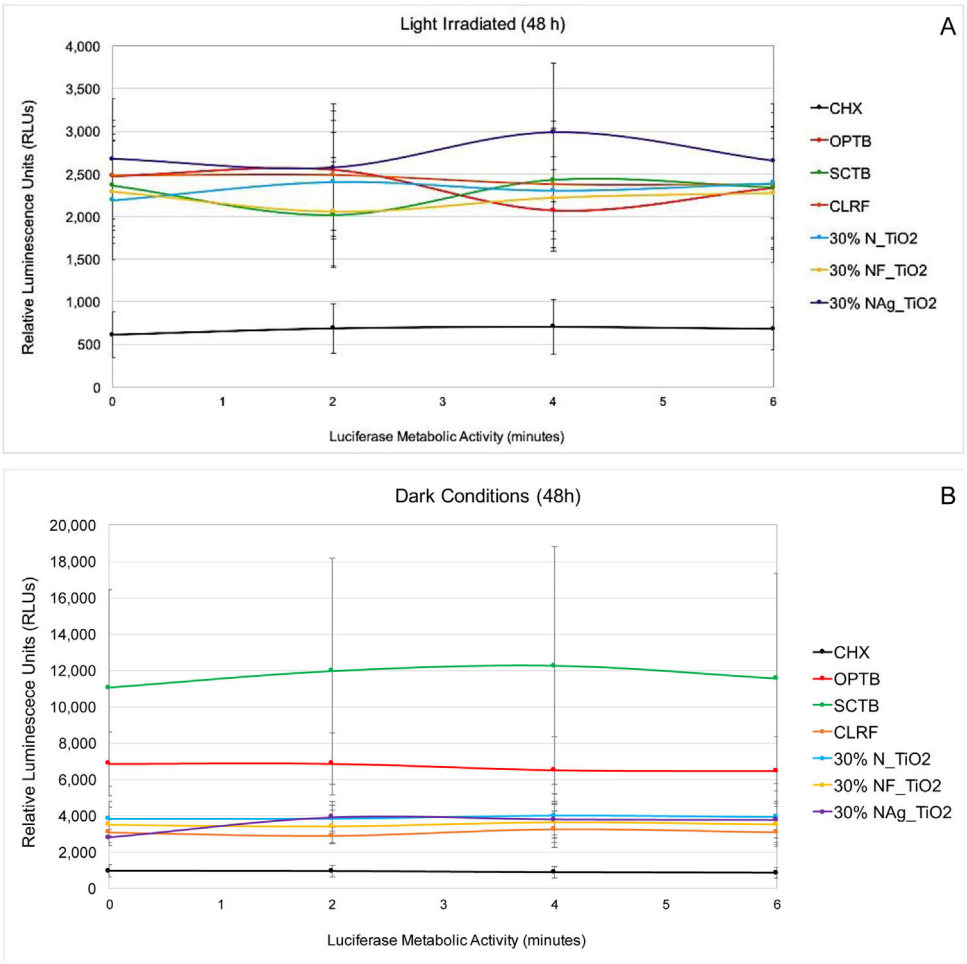

Fig. 5 –.

Viability of 48-h intact *S. mutans* biofilms grown against the surfaces of both unaltered and experimental dental adhesive resins containing 30% (v/v) of either doped or co-doped metaloxide nanoparticles (A) with or (B) without continuous light irradiation.

Table 1 –

Experimental groups and growth conditions investigated during the optimization of the high-throughput bioluminescence assay.

Experimental groups	Media []	Sucrose [%]	Dilution	Inoculum volume (μL)	Inoculum:D- Luciferin ratio (v/v)	Growth (h)	Luminescence wavelength (nm)
G1 (n = 6/growth condition, total = 3456)	0.35x	0.1	1:500	300	5:1	24	530
	0.65x		1:250	500	2:1	48	590
	1x		1:100	750			
			1:50	1000			
G2 (n = 6/growth condition, total = 3456)	0.35x	0.5	1:500	300	5:1	24	530
	0.65x		1:250	500	2:1	48	590
	1x		1:100	750			
			1:50	1000			
G3 (n = 6/growth condition, total = 3456)	0.35x	1.0	1:500	300	5:1	24	530
	0.65x		1:250	500	2:1	48	590
	1x		1:100	750			
			1:50	1000			

Dent Mater. Author manuscript; available in PMC 2021 March 01.

Table 2 –

Student–Newman–Keuls ranking describing the mean values of luciferase metabolic activity (in RLUs) and distribution of statistical significance among groups investigated for (A) 0 min, (B) 2 min, (C) 4 min and (D) 6 min after the addition of D-Luciferin substrate.

A				**B**				**C**				**D**			
Means with the same letter are not significantly different				**Means with the same letter are not significantly different**				**Means with the same letter are not significantly different**				**Means with the same letter are not significantly different**			
SNK grouping	**Mean**	**N**	**GRP**	**SNK grouping**	**Mean**	**N**	**GRP**	**SNK grouping**	**Mean**	**N**	**GRP**	**SNK grouping**	**Mean**	**N**	**GRP**
A	6468.1	72	SCTB	A	6824.4	72	SCTB	A	6813.7	72	SCTB	A	6440	72	SCTB
B	4844.3	72	OPTB	B	4917.7	72	OPTB	B	4730.1	72	OPTB	B	4634.2	72	OPTB
C	3049.3	72	NF	C	3093.3	72	NTIO	C	3166.7	72	NF	C	3198.4	72	NF
C	2967.6	72	NTIO	C	2973.9	72	NAG	C	3157.2	72	NTIO	C	3064.2	72	NTIO
C	2796.8	72	CLRF	C	2904.7	72	NF	C	3024.2	72	NAG	C	2999.5	72	NAG
C	2647.8	72	NAG	C	2713.1	72	CLRF	C	2768.2	72	CLRF	C	2772.9	72	CLRF
D	869	72	CHX	D	837.6	72	CHX	D	762.5	72	CHX	D	692	72	CHX

Table 3 –

Student–Newman–Keuls describing the mean values of luciferase metabolic activity (in RLUs) and distribution of statistical significance among groups investigated for (A) 0 min, (B) 2 min, (C) 4 min and (D) 6 min after the addition of D-Luciferin substrate.

(A) Means with the same letter are not signficantly different			
SNK grouping	Mean	N	GRP
A	6468.1	72	SCTB
B	4844.3	72	OPTB
C	3049.3	72	NF
C			
C	2967.6	72	NTIO2
C			
C	2796.8	72	CLRF
C			
C	2647.8	72	NAG
	869	72	CHX
(B) Means with the same letter are not signficantly different			
SNK grouping	Mean	N	GRP
A	6824.4	72	SCTB
B	4917.7	72	OPTB
C	3093.3	72	NTIO2
C			
C	2973.9	72	NAG
C			
C	2904.7	72	NF
C			
C	2713.1	72	CLFR
D	837.6	72	CHX
(C) Means with the same letter are not signficantly different			
SNK grouping	Mean	N	GRP
A	6813.7	72	SCTB
B	4730.1	72	OPTB
C	3166.7	72	NF

C			
C	3157.2	72	NTIO2
C			
C	3024.2	72	NAG
C			
C	2768.2	72	CLRF
D	762.5	72	CHX

(D) Means with the same letter are not signficantly different

SNK grouping	Mean	N	GRP
A	6440	72	SCTB
B	4634.2	72	OPTB
C	3198.4	72	NF
C			
C	3064.2	72	NTIO2
C			
C	2999.5	72	NAG
C			
C	2772.9	72	CLRF
D	692	72	CHX